

# Dissipative fluid dynamics for the dilute Fermi gas at unitarity: Anisotropic fluid dynamics

M. Bluhm and T. Schäfer

*Department of Physics, North Carolina State University, Raleigh, NC 27695*

## Abstract

We consider the time evolution of a dilute atomic Fermi gas after release from a trapping potential. A common difficulty with using fluid dynamics to study the expansion of the gas is that the theory is not applicable in the dilute corona, and that a naive treatment of the entire cloud using fluid dynamics leads to unphysical results. We propose to remedy this problem by including certain non-hydrodynamic degrees of freedom, in particular anisotropic components of the pressure tensor, in the theoretical description. We show that, using this method, it is possible to describe the crossover from fluid dynamics to ballistic expansion locally. We illustrate the use of anisotropic fluid dynamics by studying the expansion of the dilute Fermi gas at unitarity using different functional forms of the shear viscosity, including a shear viscosity which is solely a function of temperature,  $\eta \sim (mT)^{3/2}$ , as predicted by kinetic theory in the dilute limit.

## I. INTRODUCTION

Considerable effort has been devoted to extracting transport properties, in particular the shear viscosity and the spin diffusion constant, of dilute atomic Fermi gases [1–9]. The interest in these experiments is driven by the observation that strongly correlated Fermi gases can serve as model systems for other quantum many body systems, such as high  $T_c$  superconductors or the quark-gluon plasma [10–12]. There are, however, two difficulties that have prevented truly model independent measurements of transport coefficients in trapped systems so far. The first difficulty is that the diffusion constants for momentum or spin depend on the local density while the associated experimental observables are global measures such as the mean square cloud size or the total spin current. This implies the need to unfold the experimental data in order to obtain the density and temperature dependence of the transport coefficients. The analogous deconvolution problem for equilibrium quantities has been overcome using a number of techniques [13, 14], but the first study attempting to determine the local shear viscosity only appeared recently [9].

The second, more serious, difficulty is that the diffusion approximation breaks down in the dilute part of the cloud. This problem cannot be ignored, because a naive application of the Navier-Stokes or the diffusion equation to the dilute corona leads to paradoxical behavior. Consider, for example, a scale invariant Fermi gas expanding after release from a harmonic trap [15]. In the case of a vanishing shear viscosity the expansion dynamics is described by an exact scaling solution of the Euler equation. This solution corresponds to a Hubble-like flow, in which the fluid velocity  $\vec{u}$  is always linearly proportional to the distance from the center of the trap, and the temperature is only a function of time. We can now study how this picture is modified in the presence of a small dissipative term. The viscous contribution to the stress tensor,

$$\delta\Pi_{ij} = -\eta \left( \nabla_i u_j + \nabla_j u_i - \frac{2}{3} \delta_{ij} \vec{\nabla} \cdot \vec{u} \right), \quad (1)$$

is a constant in space that multiplies the local shear viscosity  $\eta$ . At unitarity scale invariance implies that  $\eta = n f(n/T^{2/3})$ , where  $n$  is the density,  $T$  is the temperature, and  $f(x)$  is a universal function. In the dilute limit the shear viscosity is only a function of temperature and not of density,  $\eta = \text{const} \cdot (mT)^{3/2}$ . Kinetic theory predicts  $\text{const} = 15/(32\sqrt{\pi})$  [16, 17]. Since the temperature is spatially constant one concludes that  $\delta\Pi_{ij}$  goes to a constant in the dilute part of the cloud. This implies that there is no dissipative force, but a constant

amount of dissipative heating per unit volume, where the energy for this infinite amount of heating is supplied by a heat current that flows in from spatial infinity.

This description is, of course, completely wrong. The mean free path in the dilute corona is much larger than the inter-particle spacing, and there are no collisions that could establish dissipative forces or viscous heating. Particles in the dilute corona are ballistically streaming. In order to describe the situation correctly, we have to combine a fluid dynamical description of the core with a weakly collisional theory of the corona. In this work we suggest that an efficient method for achieving this goal is to include certain non-hydrodynamic degrees of freedom, an anisotropic pressure tensor, in the theoretical description. In Section II we motivate this method by studying certain exact solutions of the Boltzmann equation. In Section III we review the derivation of standard, isotropic, fluid dynamics from kinetic theory, and in Sections IV and V we extend this method to anisotropic fluid dynamics. A similar method was proposed as an extension of fluid dynamics to describe the early stage of a heavy-ion collision, see [18, 19]. In Sections VI and VII we describe numerical methods and show results from an anisotropic fluid dynamics code. This code is a generalization of the Navier-Stokes code described in [20]. We show that our method describes the crossover from fluid dynamics to free streaming both globally, for a shear viscosity of the form  $\eta \sim n$ , and locally, for a shear viscosity of the form  $\eta \sim (mT)^{3/2}$ . We end with an outlook in Section VIII.

## II. GLOBAL CROSSOVER FROM FLUID DYNAMICS TO BALLISTIC EXPANSION

The global crossover from fluid dynamics to free streaming in the expansion of a trapped Fermi gas after release from the trap was studied in [21], based on a set of scaling solutions to the Boltzmann equation obtained in [22, 23]. We will use these solutions to motivate an extension of the fluid dynamic equations that accommodates the transition from fluid dynamics to free streaming locally. This approach is described in Sect. IV.

The scaling solutions introduced in [22, 23] solve the Boltzmann equation in a harmonic confinement potential and using the Bhatnagar-Gross-Krook (BGK) approximation. This approximation is based on a collision term of the form  $C[f] = -\delta f/\tau$ , where  $\delta f$  is the deviation of the distribution function  $f$  from the local equilibrium distribution, and  $\tau$  is the

relaxation time. The authors of [21–23] further assumed that  $\tau$  is only a function of the local temperature, but not of the local density. In the case of two-dimensional traps extensions of the scaling ansatz to anharmonic confining potentials were studied in [24].

Fluid dynamics corresponds to the limit  $\tau \rightarrow 0$ , and free streaming is realized as  $\tau \rightarrow \infty$ . In both limits the Boltzmann equation is solved by a distribution function of the form [22]

$$f(\vec{x}, \vec{v}, t) = \Gamma(t) f_0(\vec{R}(t), \vec{U}(t)), \quad (2)$$

where

$$f_0(\vec{R}, \vec{U}) \sim \exp\left(-\frac{m}{2T} \sum_i [\omega_i^2 R_i^2 + U_i^2]\right) \quad (3)$$

is the initial distribution function in a harmonic potential with frequencies  $\omega_i$  and

$$\Gamma(t) = \prod_i \frac{1}{b_i(t) \theta_i(t)^{1/2}}, \quad R_i(t) = \frac{x_i}{b_i(t)}, \quad U_i(t) = \frac{v_i - u_i}{\theta_i(t)^{1/2}}, \quad \alpha_i(t) = \frac{\dot{b}_i(t)}{b_i(t)}, \quad (4)$$

with  $u_i = \alpha_i(t) x_i$  for fixed  $i$ . We note that the ansatz in Eq. (2) preserves the shape of the initial Boltzmann distribution in the cartesian directions  $i = x, y, z$ , and that  $\theta_i$  plays the role of an anisotropic scale factor for the temperature. In the free streaming limit the solution of the Boltzmann equation is

$$\theta_i(t) = \frac{1}{b_i(t)^2}, \quad b_i(t) = \left(1 + \omega_i^2 t^2\right)^{1/2}. \quad (5)$$

In the limit of ideal fluid dynamics we find  $\theta_i(t) = \bar{\theta}(t)$  with  $\bar{\theta}(t) = [\prod_i b_i(t)]^{-2/3}$ , which implies that the temperature is isotropic. The scale parameters  $b_i(t)$  are determined by

$$\ddot{b}_i(t) = \frac{\omega_i^2}{[\prod_j b_j(t)]^{2/3} b_i(t)}. \quad (6)$$

This equation can be solved analytically in the limit of late times and a strongly deformed trap,  $\omega_z = \lambda \omega_\perp$  and  $\omega_x = \omega_y = \omega_\perp$  with trap deformation  $\lambda \ll 1$ . In this case one finds  $b_\perp(t) \simeq \sqrt{3/2} \omega_\perp t$ .

Solutions for the transverse flow velocity and the density distribution in the transverse plane are shown in Fig. 1. We observe that the free streaming and fluid dynamic solutions are qualitatively similar. Transverse pressure in fluid dynamics leads to acceleration, which is reflected in the larger expansion velocity of the fluid dynamics solution in the left panel. Over time, the larger velocity shifts the peak of the density distribution to larger radii, as shown in the right panel. It is interesting to note that the velocity field at late times is the

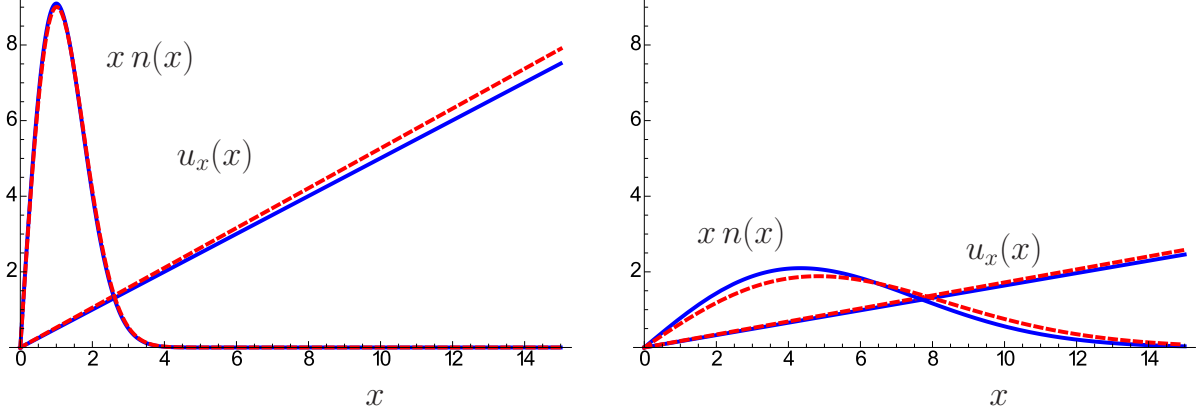


FIG. 1: Comparison between solutions of the Boltzmann equation in the limits of free streaming (blue solid curves) and ideal fluid dynamics (red dashed curves). In the left panel we show the velocity field component  $u_x$  and the transverse density profile  $xn(x)$  at an early time  $t = \omega_{\perp}^{-1}$ . In the right panel we show these observables at a later time  $t = 6\omega_{\perp}^{-1}$ . The solutions correspond to a trap deformation  $\lambda = 0.045$ . The density  $n$  and the velocity  $u_x$  are given in arbitrary units, but the scales in the left and the right panel are identical.

same in free streaming and ideal fluid dynamics. The mean velocity, that is the velocity weighted by the density, is larger in fluid dynamics because the maximum of the density is shifted to larger radii. In the limit  $\lambda \ll 1$  this difference in the mean velocity can be understood in terms of energy conservation. In free streaming the internal energy of the fluid is transferred equally to kinetic energy in all three directions. In fluid dynamics most of the energy is transferred to transverse motion, and the mean velocity is larger by a factor  $\sqrt{3/2} \simeq 1.22$ .

Figure 1 shows the difference between ideal fluid dynamics and free streaming in the idealized situation that the relaxation time is not a function of density, so that the entire cloud is either in the ballistic or the fluid dynamical regime. In reality a transition between the two regimes occurs in the dilute part of the cloud, and the transition region may shift during the evolution. In Sect. IV we will study a theoretical approach that can dynamically, as a function of time and the spatial coordinates, accommodate the crossover from fluid dynamical to ballistic behavior.

### III. FLUID DYNAMICS FROM KINETIC THEORY

Before we introduce anisotropic fluid dynamics we review the derivation of standard fluid dynamics from kinetic theory. We can view fluid dynamics as an effective description of a fluid that arises from the Boltzmann equation in the limit of a short mean free path. Consider the Boltzmann equation

$$\left(\partial_t + \vec{v} \cdot \vec{\nabla}_x - \vec{F} \cdot \vec{\nabla}_p\right) f_p(\vec{x}, t) = C[f_p], \quad (7)$$

where  $f_p$  is the single-particle distribution function,  $C[f_p]$  is the collision term,  $\vec{v} = \vec{\nabla}_p E_p$  the velocity of a particle with energy  $E_p$ , and  $\vec{F} = -\vec{\nabla}_x E_p$  is a force. Using the properties of the collision term, in particular the conservation of particle number, energy and momentum, we can derive conservation laws for the conserved currents. Taking moments of the Boltzmann equation we find (the repeated index  $j$  is summed over)

$$\begin{aligned} \frac{\partial \rho}{\partial t} + \vec{\nabla} \cdot \vec{\pi} &= 0, \\ \frac{\partial \pi_i}{\partial t} + \nabla_j \Pi_{ij} &= 0, \\ \frac{\partial \mathcal{E}}{\partial t} + \vec{\nabla} \cdot \vec{j}^{\mathcal{E}} &= 0. \end{aligned} \quad (8)$$

The conserved charges, the mass density  $\rho = mn$ , the momentum density  $\vec{\pi}$ , and the energy density  $\mathcal{E}$ , are given by

$$\begin{aligned} \rho(\vec{x}, t) &= \int d\Gamma_p m f_p(\vec{x}, t), \\ \vec{\pi}(\vec{x}, t) &= \int d\Gamma_p m \vec{v} f_p(\vec{x}, t), \\ \mathcal{E}(\vec{x}, t) &= \int d\Gamma_p E_p f_p(\vec{x}, t), \end{aligned} \quad (9)$$

where  $d\Gamma_p = d^3p/(2\pi)^3$ . The momentum density  $\vec{\pi}$  is also the conserved current associated with the conservation of mass. The remaining conserved currents are the stress tensor  $\Pi_{ij}$  and the energy current  $\vec{j}^{\mathcal{E}}$ ,

$$\Pi_{ij}(\vec{x}, t) = \int d\Gamma_p p_i v_j f_p(\vec{x}, t), \quad (10)$$

$$\vec{j}^{\mathcal{E}}(\vec{x}, t) = \int d\Gamma_p E_p \left(\vec{\nabla}_p E_p\right) f_p(\vec{x}, t). \quad (11)$$

In order for Eqs. (8) and (9) to close we have to supply constitutive equations, that is explicit expressions for the conserved currents in terms of the fluid dynamical variables  $\rho$ ,  $\vec{\pi}$

and  $\mathcal{E}$ . In kinetic theory constitutive equations can be derived by expanding the distribution function around the local thermodynamic equilibrium distribution  $f_p^0$ ,

$$f_p = f_p^0 + \delta f_p^1 + \delta f_p^2 + \dots, \quad (12)$$

where

$$f_p^0 = \exp([\mu - E(|\vec{v} - \vec{u}|)]/T), \quad (13)$$

and  $\delta f_p^n$  are terms that contain  $n$ 'th order gradients of the fluid dynamical variables. The equilibrium distribution function is expressed in terms of intensive quantities, the local chemical potential  $\mu(\vec{x}, t)$ , the temperature  $T(\vec{x}, t)$ , and the fluid velocity  $\vec{u}(\vec{x}, t)$ . From Eq. (13) we can compute the conserved currents at zeroth order in the gradient expansion. We get  $\vec{\pi} = \rho \vec{u}$  and

$$\Pi_{ij} = \rho u_i u_j + P \delta_{ij}, \quad (14)$$

as well as  $\vec{j}^{\mathcal{E}} = \vec{u} \left( w + \frac{1}{2} \rho \vec{u}^2 \right)$ . Here,  $P$  is the pressure and  $w = \mathcal{E}^0 + P$  is the enthalpy density, where  $\mathcal{E}^0$  denotes the energy density in the local rest frame of the fluid,  $\mathcal{E}^0 = \mathcal{E} - \frac{1}{2} \rho \vec{u}^2$ . The conservation laws combined with Eq. (14) lead to the Euler equations of ideal fluid dynamics. The final ingredient needed to complete the description is an equation of state,  $P = P(\mathcal{E}_0, \rho)$ . Using the dispersion relation of a free particle,  $E(\vec{v}) = \frac{1}{2} m \vec{v}^2$ , we obtain  $P = \frac{2}{3} \mathcal{E}_0$ , which agrees with the exact result for a scale invariant fluid.

The local equilibrium distribution function is a solution of the Boltzmann equation at leading order in the Knudsen number  $Kn = l_{mfp}/L$ , where  $l_{mfp}$  is the mean free path and  $L$  is the characteristic distance over which the conserved charges vary. At next order a solution can be found most easily by using a very simple form of the collision term. Using the BGK collision term

$$C[f_p] = -\frac{f_p - f_p^0}{\tau}, \quad (15)$$

and, again, taking the dispersion relation to be that of a free particle, we find

$$\delta f_p^1 = -\frac{m\tau f_p^0}{2T} \left( c_i c_j \sigma_{ij} + \left[ \frac{5T}{m} - c^2 \right] c_k q_k \right), \quad (16)$$

where we have defined  $\vec{c} = \vec{v} - \vec{u}$ , and repeated indices  $i, j, k$  are summed over. We have also introduced the strain tensor

$$\sigma_{ij} = \nabla_i u_j + \nabla_j u_i - \frac{2}{3} \delta_{ij} \vec{\nabla} \cdot \vec{u}, \quad (17)$$

as well as  $\vec{q} = -\vec{\nabla} \log(T)$ . The corresponding corrections to the conserved currents are

$$\delta \Pi_{ij} = -\eta \sigma_{ij}, \quad \delta j_i^{\mathcal{E}} = u_j \delta \Pi_{ij} - \kappa \nabla_i T, \quad (18)$$

where we have defined the shear viscosity  $\eta = \tau P$  and the thermal conductivity  $\kappa = \frac{5}{2} \tau P$ . Incorporating the gradient corrections in Eq. (18) into the conservation laws leads to the Navier-Stokes equation. Note that within the approximations used here the shear viscosity and the thermal conductivity are proportional to one another, and the bulk viscosity  $\zeta$  is zero. In general,  $\eta$ ,  $\zeta$  and  $\kappa$  are independent parameters, but in a scale invariant fluid  $\zeta = 0$  is an exact result.

#### IV. ANISOTROPIC FLUID DYNAMICS FROM KINETIC THEORY

The gradient expansion fails in the dilute regime of the cloud. An obvious solution to this problem is to consider the full Boltzmann equation, see [25]. Such an approach is motivated by the observation that even though the classical Boltzmann equation is only justified in the dilute regime, it reproduces the fluid dynamical limit in the dense regime. This implies that coarse grained observables extracted from the Boltzmann equation are in fact more reliable than the kinetic theory which is used to derive them. There are, however, some difficulties with this approach. First of all, the Boltzmann equation involves a six-dimensional phase space distribution function, and is considerably more difficult to solve than the Navier-Stokes equation. Second, the transport properties are now encoded in a non-linear collision integral, which is difficult to compute from first principles, and not easy to parameterize in a way that allows for a shear viscosity which is a general function of density and temperature. And finally, it is difficult to incorporate the empirical equation of state.

An alternative approach is to use a set of fluid dynamical equations which is equivalent to the approach presented in the previous section at some fixed order in the gradient expansion, but also contains extra, non-hydrodynamic, degrees of freedom that ensure a smooth crossover to the ballistic regime. Consider

$$f_p = f_p^{an} + \delta f_p'^1 + \delta f_p'^2 + \dots, \quad (19)$$

where

$$f_p^{an} = \exp\left(\frac{\mu}{T_{le}} - \sum_a \frac{mc_a^2}{2T_a}\right), \quad T_{le} = \left(\prod_a T_a\right)^{1/3}. \quad (20)$$



The form of the anisotropic distribution function  $f_p^{an}$  is motivated by the observation that, for suitable choices of  $\mu$ ,  $T_a$  and  $u_a = v_a - c_a$  Eq. (20) is an exact solution of the Boltzmann equation describing the expansion from a harmonic trapping potential in the free streaming, collisionless limit, see Section II. In order to derive the conservation laws and constitutive equations we will use the free dispersion relation  $E_p = p^2/(2m)$ . This is sufficient in order to recover the ballistic and fluid dynamical limits, but restricts the form of the equation of state to  $P = nT = \frac{n}{3} \sum_a T_a$ . This is not a problem in the scale invariant limit, because the evolution equations are only sensitive to the relation  $P(\mathcal{E}^0) = \frac{2}{3}\mathcal{E}^0$ , which is fixed by scale invariance. The full equation of state,  $P = P(n, T)$ , is needed to determine the initial density profile from the equation of hydrostatic equilibrium,  $\vec{\nabla}P = -n\vec{\nabla}V$ , where  $V$  is the confining potential.

We note that the ansatz for  $f_p^{an}$  breaks rotational invariance. This particular ansatz is intended for analyzing the expansion of a gas cloud from a harmonic confinement potential, where the symmetry axes of the potential are aligned with the cartesian coordinate system used. Rotational symmetry can be restored by using the more general ansatz

$$f_p^{an} = \exp\left(\frac{\mu}{T_{le}} - \sum_{a,b} \frac{m}{2} c_a \theta_{ab} c_b\right), \quad T_{le} = \left(\det(\theta^{-1})\right)^{1/3}. \quad (21)$$

For our purposes we will continue to use the simpler ansatz given in Eq. (20).

We can use Eqs. (9) - (11) to determine the constitutive equations. We find  $\vec{\pi} = \rho\vec{u}$  and

$$\mathcal{E} = \frac{1}{2}\rho\vec{u}^2 + \mathcal{E}^0, \quad \mathcal{E}^0 = \frac{3}{2}P. \quad (22)$$

The stress tensor is given by

$$\Pi_{ij} = \rho u_i u_j + P\delta_{ij} + \delta\Pi_{ij}, \quad \delta\Pi_{ij} = \delta_{ia}\delta_{ja}\Delta P_a, \quad (23)$$

where  $\Delta P_a = P_a - P$ . We use the convention that repeated vector indices  $i, j, k$  are summed over, but repeated anisotropic indices  $a, b$  are not, unless an explicit summation symbol occurs. The components of the energy current are

$$j_i^{\mathcal{E}} = u_i \left(\frac{1}{2}\rho\vec{u}^2 + w\right) + \delta j_i^{\mathcal{E}}, \quad \delta j_i^{\mathcal{E}} = u_j \delta\Pi_{ij} = \delta_{ia} u_a \Delta P_a, \quad (24)$$

where  $w = \mathcal{E}^0 + P$ . In kinetic theory we also find  $P = nT$  and  $P_a = nT_a$ . Combining the constitutive equations (22) - (24) with the conservation laws Eqs. (8) and (9) gives five

equations for seven fluid dynamical variables,  $\mu$ ,  $P_a$  and  $u_i$ . We can get two additional equations by considering further moments of the Boltzmann equation. The conservation laws arise from taking moments with respect to the conserved quantities 1,  $m\vec{v}$ , and  $m\vec{v}^2/2$ . Taking moments with  $mv_a^2/2$  (no sum over  $a$ ) gives

$$\frac{\partial \mathcal{E}_a}{\partial t} + \vec{\nabla} \cdot \vec{j}_a^\mathcal{E} = -\frac{\Delta P_a}{2\tau}, \quad (25)$$

where we have defined

$$\mathcal{E}_a = \frac{1}{2}\rho u_a^2 + \mathcal{E}_a^0, \quad (26)$$

$$(j_a^\mathcal{E})_i = u_i \left( \frac{1}{2}\rho u_a^2 + \mathcal{E}_a^0 + \delta_{ia}P \right) + (\delta j_a^\mathcal{E})_i, \quad (27)$$

and  $\mathcal{E}_a^0 = \frac{1}{2}P_a$  as well as

$$(\delta j_a^\mathcal{E})_i = \delta_{ia}u_j \delta \Pi_{ij} = \delta_{ia}u_a \Delta P_a. \quad (28)$$

Note that Eq. (25), when summed over  $a$ , gives the equation of energy conservation. The remaining two equations determine the non-equilibrium pressure components  $P_a$ . Also note that we can derive additional equations based on the off-diagonal moments with  $mv_a v_b/2$  ( $a \neq b$ ). These equations determine the off-diagonal components of the temperature in Eq. (21).

We will show in Section V that Eq. (23) reduces to the Navier-Stokes stress tensor in the limit  $\tau \rightarrow 0$ . This implies that  $f_p^{an}$  already contains all terms of order  $\mathcal{O}(\nabla_i u_j)$  in  $\delta f_p^1$ , and that  $\delta f_p'^1$  only includes terms associated with heat conduction,  $\delta f_p'^1 = \mathcal{O}(\nabla_i T)$ . It is straightforward to include these effects, but in the context of an expanding gas cloud heat conduction is a very small effect, because the initial state is isothermal and this property is preserved by the evolution in ideal fluid dynamics. This implies that gradients of the temperature are proportional to  $\tau$ , and, thus, heat flow is a second order effect in the relaxation time,  $\kappa \nabla_i T = \mathcal{O}(\tau^2)$ .

## V. FLUID DYNAMICAL EQUATIONS IN LAGRANGIAN FORM

In practice we solve the equations of fluid dynamics in Lagrangian form. We introduce the comoving time derivative  $D_0 = \partial_0 + \vec{u} \cdot \vec{\nabla}$ . The continuity equation can be written as

$$D_0 \rho = -\rho \vec{\nabla} \cdot \vec{u} \quad (29)$$

and the equations of momentum and energy conservation are

$$D_0 u_i = -\frac{1}{\rho} (\nabla_i P + \nabla_j \delta \Pi_{ij}) , \quad (30)$$

$$D_0 \epsilon = -\frac{1}{\rho} \nabla_i (u_i P + \delta j_i^\mathcal{E}) , \quad (31)$$

where we have defined the energy per mass  $\epsilon = \mathcal{E}/\rho$  and  $\delta j_i^\mathcal{E} = u_j \delta \Pi_{ij}$  as well as  $\delta \Pi_{ij} = \delta_{ia} \delta_{ja} \Delta P_a$ . The equation for the anisotropic energy density can be written as

$$D_0 \epsilon_a = -\frac{1}{\rho} \nabla_i [\delta_{ia} u_i P + (\delta j_a^\mathcal{E})_i] - \frac{1}{2\tau\rho} \Delta P_a , \quad (32)$$

where  $\epsilon_a = \mathcal{E}_a/\rho$  and  $(\delta j_a^\mathcal{E})_i = \delta_{ia} u_j \delta \Pi_{ij}$ . In standard fluid dynamics we view  $\rho$ ,  $u_i$  and  $\mathcal{E}$  as the fluid dynamical variables. Their time evolution is governed by Eqs. (29) - (31), and in order to determine the RHS of Eqs. (30) and (31) we use the equation of state  $P(\mathcal{E}^0)$  with  $\mathcal{E}^0 = \mathcal{E} - \frac{1}{2}\rho \vec{u}^2$ , where in a scale invariant fluid  $P(\mathcal{E}^0) = \frac{2}{3}\mathcal{E}^0$ . In anisotropic fluid dynamics we have two extra variables,  $\mathcal{E}_1$  and  $\mathcal{E}_2$  with  $\sum_a \mathcal{E}_a = \mathcal{E}$ . Their time evolution is governed by Eq. (32), and  $P_a$  is given by the anisotropic equation of state  $P_a(\mathcal{E}_a^0) = 2\mathcal{E}_a^0$  with  $\mathcal{E}_a^0 = \mathcal{E}_a - \frac{1}{2}\rho u_a^2$ . Note that  $P = \frac{1}{3} \sum_a P_a$  satisfies the isotropic equation of state.

In the previous section we argued that in the limit  $\tau \rightarrow 0$  anisotropic fluid dynamics reduces to Navier-Stokes viscous fluid dynamics. We expect, in particular, that the dissipative correction to the stress tensor  $\delta \Pi_{ij} = \delta_{ia} \delta_{ja} \Delta P_a$  approaches  $\delta \Pi_{ij} = -\eta \sigma_{ij}$  (for  $i = j$ ) with  $\eta = \tau P$ . To see this we rewrite Eq. (32) as

$$\Delta P_a = -2\tau\rho \left( D_0 \epsilon_a + \frac{1}{\rho} \nabla_i [\delta_{ia} u_i P + (\delta j_a^\mathcal{E})_i] \right) \quad (33)$$

and solve for  $\Delta P_a$  at leading order in  $\tau$ . This implies that in evaluating  $\mathcal{E}_a^0$  and  $(\delta j_a^\mathcal{E})_i$  we can replace  $P_a$  by  $P$ , so that  $\epsilon_a = \frac{1}{3}\epsilon - \frac{1}{6}\vec{u}^2 + \frac{1}{2}u_a^2$  and  $(\delta j_a^\mathcal{E})_i = 0$ . We use the equations of ideal fluid dynamics to compute  $D_0 \epsilon$  and  $D_0 u_i$  and find

$$\Delta P_a = \tau P \left( \frac{2}{3} \vec{\nabla} \cdot \vec{u} - 2 \nabla_a u_a \right) + \mathcal{O}(\tau^2) = -\tau P \sigma_{aa} + \mathcal{O}(\tau^2) . \quad (34)$$

This result shows that anisotropic fluid dynamics relaxes to the Navier-Stokes equation with

$$\eta = \tau P , \quad (35)$$

where  $\tau$  is the relaxation time. Note that the expression in Eq. (23) does not reproduce the off-diagonal components of  $\delta \Pi_{ij}$  in Navier-Stokes theory. In order to study flows in which these terms are non-zero we have to start from the more general ansatz in Eq. (21) and consider moments of the Boltzmann equation with  $mv_a v_b/2$  for  $a \neq b$ .

## VI. ANISOTROPIC FLUID DYNAMICS: NUMERICAL METHOD AND CHOICE OF UNITS

We have implemented anisotropic fluid dynamics as an extension of the Navier-Stokes code described in [20]. The Navier-Stokes code solves the advection equations in Lagrangian coordinates. A Lagrangian time step is followed by a piecewise parabolic remap onto an Eulerian grid. The algorithm is based on the PPMLR (Piecewise-Parabolic Method, Lagrangian-Remap) scheme developed by Colella and Woodward [26] and implemented as a multi-dimensional method in the VH1 code written by Blondin and Lufkin [27]. The main modification is that we add the fluid dynamical variables  $P_a$  and  $\mathcal{E}_a$  and solve Eq. (32). We solve for all three components of  $P_a$  and verify that  $\frac{1}{3}\sum_a P_a$  agrees with  $P$ . Since Eq. (32) is a relaxation equation for  $\Delta P_a$  we have to choose the time step as

$$\Delta t = \min \left( c_s \frac{\Delta x}{2}, u_i \frac{\Delta x}{2}, \tau \right), \quad (36)$$

where  $c_s$  is the local speed of sound,  $\Delta x$  is the grid spacing, and  $\tau = \eta/P$  is the local relaxation time. The first two constraints arise from the condition that disturbances emerging from opposite faces of a fluid cell cannot interact during a time step. The third constraint ensures that the relaxation time equation is stable. The condition  $\Delta t \leq \tau$  implies that the simulation becomes inefficient if  $\tau$  is very small, which is close to the limit of ideal fluid dynamics. In principle this can be addressed by using the analytic result given in Eq. (34), but we have not done so in the present work.

We have studied the evolution of a unitary Fermi gas after release from a harmonic trap. The trapping potential is  $V(x) = \frac{1}{2}m\omega_i^2 x_i^2$  with  $\omega_x = \omega_y = \omega_\perp$  and  $\omega_z = \lambda\omega_\perp$ . We use dimensionless variables for distance, time and velocity based on the following system of units [20]

$$x_0 = (3N\lambda)^{1/6} \left( \frac{2}{3m\omega_\perp} \right)^{1/2}, \quad t_0 = \omega_\perp^{-1}, \quad u_0 = x_0\omega_\perp. \quad (37)$$

The unit of density is  $n_0 = x_0^{-3}$ . The corresponding units for energy density, pressure, and temperature are given by

$$\mathcal{E}_0 = \frac{m\omega_\perp^2}{x_0}, \quad P_0 = \frac{m\omega_\perp^2}{x_0}, \quad T_0 = m\omega_\perp^2 x_0^2. \quad (38)$$

Finally, the unit of the shear viscosity is

$$\eta_0 = \frac{m\omega_\perp}{x_0}. \quad (39)$$

In the high temperature limit the initial density is a Gaussian. The central density is given by

$$n(0) = n_0 \frac{N\lambda}{\pi^{3/2}} \left( \frac{E_F}{E_0} \right)^{3/2}, \quad (40)$$

where  $N$  is the number of particles,  $E_F = (3N\lambda)^{1/3}\omega_\perp$  is the Fermi energy, and  $E_0$  is the total energy per particle of the trapped gas. Moreover, it is convenient to normalize the dimensionless central density  $n(0)/n_0$  to one. This means we also divide the density by the dimensionless factor  $(N\lambda)/\pi^{3/2} \cdot (E_F/E_0)^{3/2}$  in equ. (40). The normalized dimensionless shear viscosity is

$$\bar{\eta} = \frac{\eta}{\eta_0} \frac{n_0}{n(0)}. \quad (41)$$

In the following we will consider a shear viscosity of the form  $\eta = \alpha_n n + \alpha_T (mT)^{3/2}$ . The corresponding dimensionless shear viscosity is  $\bar{\eta} = \bar{\alpha}_n \bar{n} + \bar{\alpha}_T \bar{T}^{3/2}$  with

$$\bar{\alpha}_n = \frac{3}{2} \frac{\alpha_n}{(3N\lambda)^{1/3}}, \quad \bar{\alpha}_T = \frac{4\pi^{3/2}}{3} \frac{\alpha_T}{(3N\lambda)^{1/3}} \left( \frac{E_0}{E_F} \right)^{3/2}. \quad (42)$$

Kinetic theory predicts that in the high temperature limit  $\alpha_n = 0$  and  $\alpha_T = 15/(32\sqrt{\pi})$ . In the anisotropic fluid dynamics framework the shear viscosity is determined by the relaxation time. The dimensionless relaxation time is

$$\bar{\tau} = \frac{\tau}{t_0} = \frac{\bar{\eta}}{\bar{P}}. \quad (43)$$

Equation (42) shows that, in dimensionless units, the number of particles  $N$  only appears together with the viscosity coefficient. This implies that the ideal evolution is independent of  $N$ , and that for a given viscosity dissipative effects are smaller for a larger number of particles.

## VII. ANISOTROPIC FLUID DYNAMICS: RESULTS

We first consider the case  $\alpha_T = 0$  and study the dependence on  $\alpha_n$ . Figure 2 shows the time evolution of the aspect ratio  $A_R(t) = \langle r_\perp^2 \rangle / \langle r_z^2 \rangle$ , defined by the ratio of mean squared transverse and longitudinal cloud radii, for different values of the shear viscosity,  $\bar{\alpha}_n = 0.1, 1, 1000$ . For comparison we also show the result in ideal fluid dynamics, the free streaming limit, and the solution of the Navier-Stokes equation for  $\bar{\alpha}_n = 0.1, 1$ . We consider a Gaussian initial condition, which corresponds to a solution of the hydrostatic equation in

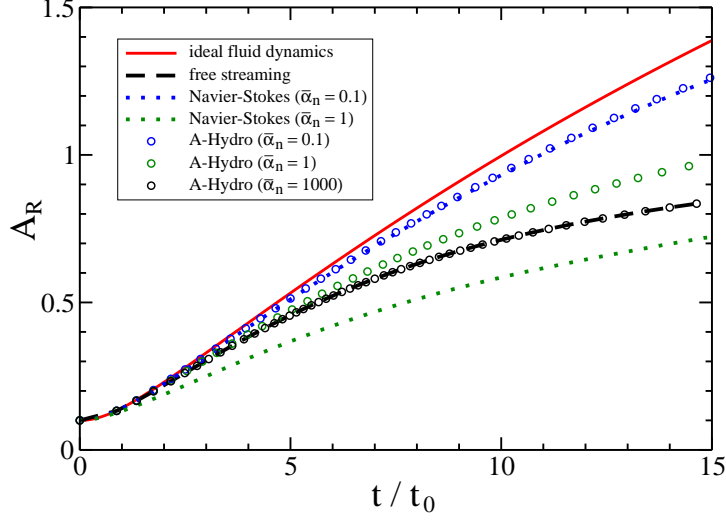


FIG. 2: This figure shows the evolution of the aspect ratio  $A_R$  as a function of time  $t$  in dimensionless units, as explained in the text. The initial trap deformation is  $A_R(0) = \lambda = 0.1$  and the initial energy is  $E_0/E_F = 1$ . The red solid curve shows the evolution in ideal fluid dynamics, and the black dashed curve is the free streaming limit. The remaining curves were obtained using viscous fluid dynamics with different values of  $\bar{\alpha}_n$  for the shear viscosity  $\bar{\eta} = \bar{\alpha}_n \bar{n}$ . The dotted curves show Navier-Stokes results for  $\bar{\alpha}_n = 0.1, 1$  and the data points are the corresponding predictions from anisotropic fluid dynamics. In the case of anisotropic fluid dynamics we also show the result for  $\bar{\alpha}_n = 1000$ , which is close to the free streaming limit.

the case of an equation of state of a free gas,  $P = nT$ . At  $t = 0$  the aspect ratio is given by the trap deformation,  $A_R(0) = \lambda$ . Pressure gradients preferentially accelerate the fluid in the transverse direction, and  $A_R(t)$  grows as a function of time. Viscous effects counteract the expansion in the transverse direction, and accelerate the fluid in the longitudinal direction, reducing the value of  $A_R(t)$ .

For the smallest value of the shear viscosity,  $\bar{\alpha}_n = 0.1$ , we find good agreement between anisotropic fluid dynamics and Navier-Stokes theory, as expected from Eq. (34). For larger values of  $\bar{\alpha}_n$  anisotropic fluid dynamics predicts that dissipative effects saturate, and that  $A_R(t)$  approaches the free streaming limit. In Navier-Stokes theory, on the other hand, dissipative effects continue to grow with  $\bar{\alpha}_n$  and the evolution of  $A_R(t)$  becomes arbitrarily slow.

More details are provided by Fig. 3. In this figure, we compare the dissipative corrections

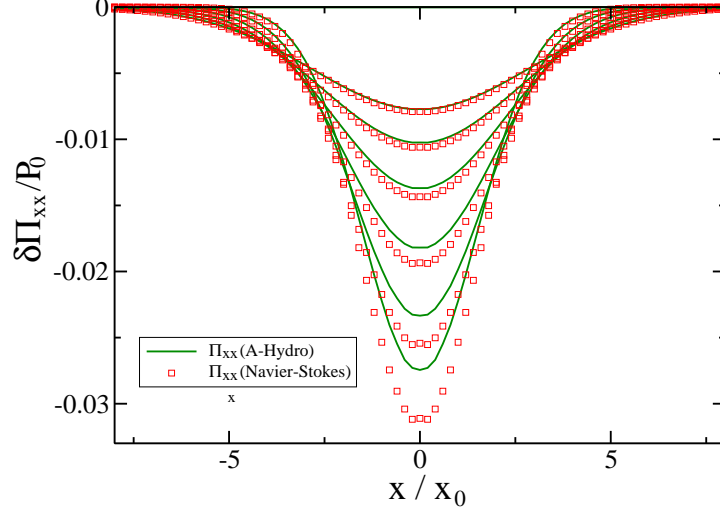


FIG. 3: This figure shows the  $xx$  component of the dissipative correction to the stress tensor  $\delta\Pi_{xx}(x,0,0)$  in Navier-Stokes theory (green solid curve) and in anisotropic fluid dynamics (red squares) for different times  $t/t_0 = 0.75 - 2.0$  in steps of  $\Delta t = 0.25 t_0$ . The magnitude of the viscous stresses decreases with time. The calculation was performed with a density dependent shear viscosity  $\bar{\eta} = \bar{\alpha}_n \bar{n}$  and  $\bar{\alpha}_n = 0.15$ . We used a trap deformation  $\lambda = 0.045$  and an initial energy  $E_0/E_F = 3$ .

to the stress tensor in Navier-Stokes theory and in anisotropic fluid dynamics. We focus on the  $xx$  components  $\delta\Pi_{xx}^{NS} = -\eta\sigma_{xx}$  and  $\delta\Pi_{xx}^{AH} = \Delta P_x$  at different times during the evolution of the expanding gas cloud. The calculation was performed for  $\bar{\alpha}_n = 0.15$ , so that the aspect ratio  $A_R(t)$  shows good agreement between Navier-Stokes theory and anisotropic fluid dynamics. Note that  $\delta\Pi_{xx}^{NS}$  in Fig. 3 was computed using the velocity field in anisotropic fluid dynamics. We observe that the two dissipative stress tensors are indeed very close, and that the agreement improves at late times. This indicates that the equations of anisotropic fluid dynamics contain second order terms in  $\tau$  that describe the relaxation of the stress tensor to the Navier-Stokes limit [28, 29].

Figure 4 demonstrates that anisotropic fluid dynamics can be applied to the case of a purely temperature dependent shear viscosity,  $\eta = \alpha_T(mT)^{3/2}$ , for which Navier-Stokes fluid dynamics fails. We observe that in the center of the cloud the two dissipative corrections to the stress tensor are close, in particular at late times. In the corona, however,  $\delta\Pi_{xx}^{NS}$  and  $\delta\Pi_{xx}^{AH}$  are very different. As explained in Section I the dissipative contribution to the

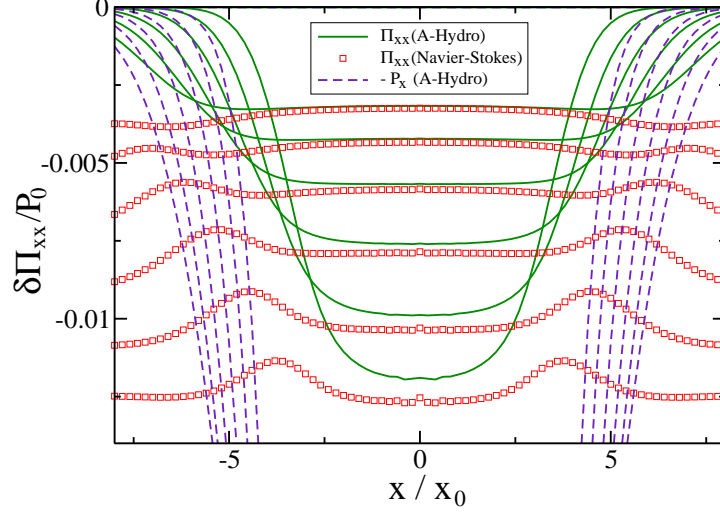


FIG. 4: Same as Fig. 3 for a temperature dependent shear viscosity  $\bar{\eta} = \bar{\alpha}_T \bar{T}^{3/2}$  with  $\bar{\alpha}_T = 0.06$ . The blue dashed line shows the negative of the anisotropic pressure component  $P_x$ .

Navier-Stokes stress tensor is approximately constant in space. In contrast, the dissipative contribution to the stress tensor in anisotropic fluid dynamics goes to zero in the dilute part of the cloud. As we can see from the blue dashed curves in Fig. 4 this happens in the regime where the dissipative stresses are comparable to the total pressure of the fluid,  $|\delta\Pi_{xx}^{NS}| \sim P_x$ . This condition, corresponding to the point where the dashed blue line intersects the red symbols, signals the breakdown of Navier-Stokes theory.

We note that  $-\nabla_x \delta\Pi_{xx}^{AH}$  corresponds to a force that points towards the center of the cloud, and reduces the transverse expansion. We also observe that at late times  $\sigma_{xx}$ , which measures the slope of the velocity field, is smaller in the center than in the corona. Viscous forces push on the center of the cloud and slow it down, while the ballistic corona is lifting off.

In anisotropic fluid dynamics the viscous stresses are concentrated in the center of the gas cloud even if  $\eta\sigma_{ij}$  is not localized. We therefore expect that the time evolution of the aspect ratio  $A_R(t)$  can be described by an effective density dependent shear viscosity  $\eta \sim n$  even if the microscopic shear viscosity is only a function of temperature. This approximation has been used to analyze experimental data on the expansion of trapped Fermi gases near unitarity [4, 8]. In Fig. 5 we show that for a given initial temperature, and for a suitably chosen value of  $\alpha_n$ , the evolution of  $A_R(t)$  is indeed essentially indistinguishable between



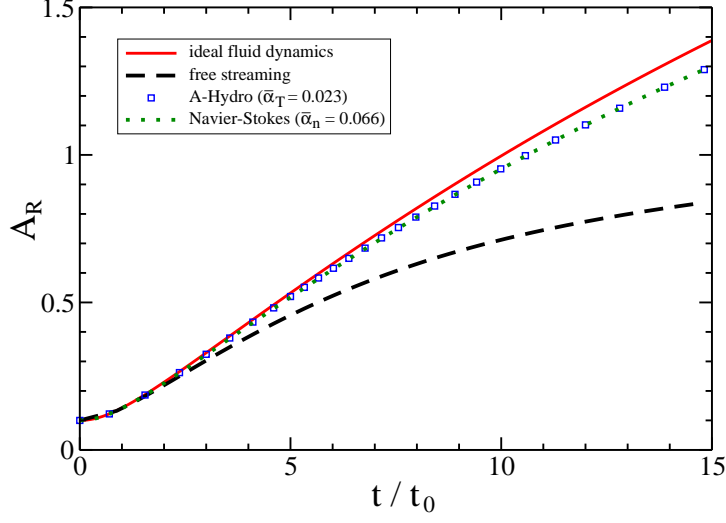


FIG. 5: This figure shows the time evolution of the aspect ratio  $A_R$  from a simulation using anisotropic fluid dynamics with  $\bar{\alpha}_T = 0.023$  in  $\bar{\eta} = \bar{\alpha}_T \bar{T}^{3/2}$  and  $\lambda = 0.1$ ,  $E_0/E_F = 1$  (blue squares). For comparison we also show the result in ideal fluid dynamics (red solid curve) and the case of purely ballistic expansion (black dashed curve). The green dotted curve shows a fit to the  $\bar{\alpha}_T = 0.023$  result based on Navier-Stokes theory with  $\bar{\alpha}_n = 0.066$  in  $\bar{\eta} = \bar{\alpha}_n \bar{n}$ .

the two cases  $\eta \sim n$  and  $\eta \sim (mT)^{3/2}$ .

In order to resolve this ambiguity and determine the full microscopic dependence of  $\eta$  on  $n$  and  $T$  we have to study the sensitivity of the effective  $\alpha_n$  on the initial temperature  $T$  or the initial energy  $E_0/E_F$ . In the literature, the value of  $\alpha_n$  which describes the time evolution of  $A_R(t)$  at a given initial temperature is referred to as the trap averaged value of  $\eta/n$ , denoted  $\langle \alpha_n \rangle$  [4]. In Fig. 6 we show the dependence of  $\langle \alpha_n \rangle$  on  $E_0/E_F$  for the case  $\eta = 15/(32\sqrt{\pi})(mT)^{3/2}$ . We consider a Gaussian initial condition, so that  $E_0 = 3T$ . We observe that the growth of  $\langle \alpha_n \rangle$  is not simply proportional to  $E_0^{3/2}$ . This is because the evolution is not only sensitive to the temperature dependence of the shear viscosity,  $\eta \sim T^{3/2}$ , but also to the temperature dependence of the relaxation time,  $\tau \sim T^{1/2}$ , and the temperature dependence of the effective relaxation volume.

We note that as a consequence of the complicated dependence of  $\langle \alpha_n \rangle$  on the system size and lifetime the result is not universal, which means that  $\langle \alpha_n \rangle$  depends on the number of particles  $N$  and the trap deformation  $\lambda$ . In the present work we will not attempt to perform a detailed analysis of the experimental data obtained in [8, 9]. This will require implementing

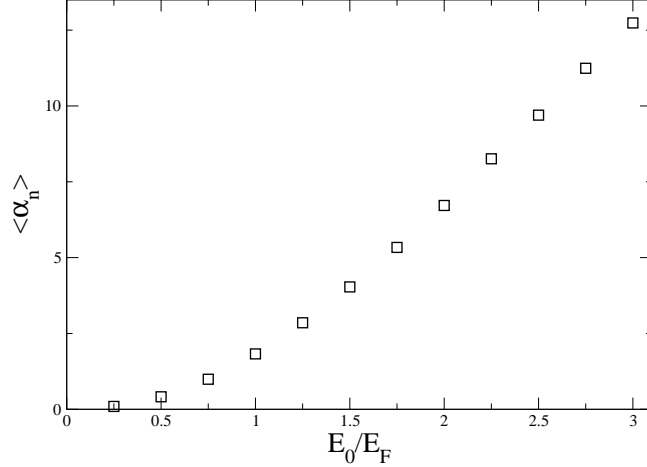


FIG. 6: This figure shows the dependence of  $\langle \alpha_n \rangle$ , the effective trap averaged ratio  $\eta/n$ , on the initial energy per particle in units of the Fermi energy  $E_F$ . A precise definition of  $\langle \alpha_n \rangle$  is given in the text. The calculation was performed for a gas cloud of  $2 \cdot 10^5$  particles with an initial trap deformation of  $\lambda = 0.045$ . The microscopic shear viscosity is given by the kinetic theory result in the high temperature limit,  $\eta = 15/(32\sqrt{\pi})(mT)^{3/2}$ .

a non-axially symmetric confining potential, a non-Gaussian initial density distribution, a realistic equation of state  $P(n, T)$ , and a shear viscosity which is a function of both  $n$  and  $T$ . It is nevertheless interesting to consider a rough comparison between our results and the analysis in [9]. At  $E_0/E_F = 3.14$  we find  $\langle \alpha_n \rangle = 13.49$ , compared to  $\langle \alpha_n \rangle = 19.63 \pm 0.54$  reported in [9]. The discrepancy is an indication of the magnitude of the effects due to the trap geometry, contributions beyond the dilute limit of the equation of state and the shear viscosity, and possible shortcomings of our description in the regime where the size of the fluid dynamical core shrinks to zero, and a kinetic treatment of the entire cloud is more appropriate.

## VIII. CONCLUSIONS AND OUTLOOK

In this work we have shown that by including non-hydrodynamic degrees of freedom it is possible to achieve a smooth transition between fluid dynamics and the ballistic limit. There are a number of interesting applications and theoretical issues that remain to be investigated.

- Other fluid dynamic problems: The anisotropic fluid dynamics approach, described by equ. (29-32), provides a general scheme for addressing problems in which the transition regime from fluid dynamics to ballistic behavior plays a role. In this work we have applied this method to the expansion of a unitary Fermi gas from a harmonic trap, but the applicability of the approach is clearly much broader, including Bose or classical gases, as well as other experimental observables, such as collective modes.
- Restoring rotational invariance: In this work we only considered the “cartesian” ansatz in Eq. (20). In order to restore full rotational invariance we have to start from Eq. (21) and derive the corresponding fluid dynamical equations.
- Relation to second order fluid dynamics: In our numerical simulations we observed that anisotropic fluid dynamics contains some effects that appear at second order in the gradient expansion of fluid dynamics, in particular a finite viscous relaxation time. It will be interesting to make this more precise, and extend the equations of motion to complete second order accuracy.
- More accurate treatment of the Knudsen limit: We have shown that anisotropic fluid dynamics reproduces the Navier-Stokes equation at order  $\mathcal{O}(\tau)$ , where  $\tau$  is the relaxation time in the BGK approximation to the Boltzmann equation. In the opposite limit,  $\tau \rightarrow \infty$ , anisotropic fluid dynamics provides an exact solution of the Boltzmann equation for  $\tau = \infty$ . However, at  $\mathcal{O}(1/\tau)$  anisotropic fluid dynamics does not provide an exact solution of the Boltzmann equation, only a solution at second order in an expansion in moments of the distribution function with respect to momentum. The reliability of this approximation can be studied by comparing with the exact numerical solutions obtained in [25].
- Extension to superfluid hydrodynamics: The experimental results obtained in [9] also cover the regime  $T < T_c$ , where  $T_c$  is the critical temperature for superfluidity. In order to extract the shear viscosity in this regime we have to extend anisotropic fluid dynamics to the superfluid (two-fluid) regime.
- Extension to spin diffusion: The problem related to the dilute regime also affects the extraction of the spin diffusion constant. It will be interesting to study whether our method can be extended to the case of charge and spin diffusion.

Our immediate goal is to use the method developed in this work to extract the local shear viscosity  $\eta(n, T) = n f(n/T^{2/3})$  from the data presented in [9]. This can be achieved by inverting the dependence of the aspect ratio  $A_R(E_0, t)$  as a function of the initial energy on the function  $f(x)$ . As explained in the previous section, this will require implementing a non-Gaussian initial density distribution as well as considering a non-axially symmetric trap, and a realistic equation of state  $P(n, T)$ . A natural starting point for unfolding the full density and temperature dependence of the shear viscosity is the reconstruction presented in [9]. At this point we have not implemented a superfluid version of the anisotropic fluid dynamics method, and we are limited to the regime  $T > T_c$ .

Acknowledgments: This work was supported in parts by the US Department of Energy grant DE-FG02-03ER41260. We would like to thank James Joseph and John Thomas for many useful discussions. We would also like to thank John Blondin for help with the VH1 code.

- 
- [1] J. Kinast, A. Turlapov, J. E. Thomas, “Two Transitions in the Damping of a Unitary Fermi Gas,” *Phys. Rev. Lett.* **94**, 170404 (2005) [cond-mat/0502507].
  - [2] T. Schäfer, “The Shear Viscosity to Entropy Density Ratio of Trapped Fermions in the Unitarity Limit,” *Phys. Rev. A* **76**, 063618 (2007) [arXiv:cond-mat/0701251].
  - [3] A. Turlapov, J. Kinast, B. Clancy, L. Luo, J. Joseph, J. E. Thomas, “Is a Gas of Strongly Interacting Atomic Fermions a Nearly Perfect Fluid” *J. Low Temp. Phys.* **150**, 567 (2008) [arXiv:0707.2574].
  - [4] C. Cao, E. Elliott, J. Joseph, H. Wu, J. Petricka, T. Schäfer and J. E. Thomas, “Universal Quantum Viscosity in a Unitary Fermi Gas,” *Science* **331**, 58 (2011) [arXiv:1007.2625 [cond-mat.quant-gas]].
  - [5] A. Sommer, M. Ku, G. Roati, and M. W. Zwierlein. “Universal spin transport in a strongly interacting Fermi gas,” *Nature* **472**, 201 (2011) [arXiv:1103.2337v1 [cond-mat.quant-gas]].
  - [6] G. M. Bruun, C. J. Pethick, “Spin diffusion in trapped clouds of strongly interacting cold atoms,” *Phys. Rev. Lett.* **107**, 255302 (2011) [arXiv:1109.5709 [cond-mat.quant-gas]].
  - [7] M. Koschorreck, D. Pertot, E. Vogt, M. Köhl, “Universal spin dynamics in two-dimensional Fermi gases,” *Nature Physics* **9**, 405 (2013) [arXiv:1304.4980 [cond-mat.quant-gas]].

- [8] E. Elliott, J. A. Joseph, J. E. Thomas, “Anomalous minimum in the shear viscosity of a Fermi gas,” *Phys. Rev. Lett.* **113**, 020406 (2014) [arXiv:1311.2049 [cond-mat.quant-gas]].
- [9] J. A. Joseph, E. Elliott, J. E. Thomas, “Shear viscosity of a universal Fermi gas near the superfluid phase transition,” arXiv:1410.4835 [cond-mat.quant-gas].
- [10] H. Guo, D. Wulin, C.-C. Chien, K. Levin, “Perfect Fluids and Bad Metals: Transport Analogies Between Ultracold Fermi Gases and High  $T_c$  Superconductors,” *New J. Phys.* **13**, 075011 (2011) [arXiv:1009.4678 [cond-mat.supr-con]].
- [11] T. Schäfer and D. Teaney, “Nearly Perfect Fluidity: From Cold Atomic Gases to Hot Quark Gluon Plasmas,” *Rept. Prog. Phys.* **72**, 126001 (2009) [arXiv:0904.3107 [hep-ph]].
- [12] A. Adams, L. D. Carr, T. Schäfer, P. Steinberg and J. E. Thomas, “Strongly Correlated Quantum Fluids: Ultracold Quantum Gases, Quantum Chromodynamic Plasmas, and Holographic Duality,” *New J. Phys.* **14**, 115009 (2012) [arXiv:1205.5180 [hep-th]].
- [13] T.-L. Ho, Q. Zhou. “Obtaining the phase diagram and thermodynamic quantities of bulk systems from the densities of trapped gases,” *Nature Physics* **6**, 131 (2010) [arXiv:0901.0018 [cond-mat.supr-con]].
- [14] M. J. H. Ku, A. T. Sommer, L. W. Cheuk, and M. W. Zwierlein, “Revealing the Superfluid Lambda Transition in the Universal Thermodynamics of a Unitary Fermi Gas,” *Science* **335**, 563 (2012) [arXiv:1110.3309 [cond-mat.quant-gas]].
- [15] T. Schäfer and C. Chafin, “Scaling Flows and Dissipation in the Dilute Fermi Gas at Unitarity,” *Lect. Notes Phys.* **836**, 375 (2012) [arXiv:0912.4236 [cond-mat.quant-gas]].
- [16] G. M. Bruun, H. Smith, “Viscosity and thermal relaxation for a resonantly interacting Fermi gas,” *Phys. Rev. A* **72**, 043605 (2005) [cond-mat/0504734].
- [17] G. M. Bruun, H. Smith, “Shear viscosity and damping for a Fermi gas in the unitarity limit,” *Phys. Rev. A* **75**, 043612 (2007) [cond-mat/0612460].
- [18] W. Florkowski and R. Ryblewski, “Highly-anisotropic and strongly-dissipative hydrodynamics for early stages of relativistic heavy-ion collisions,” *Phys. Rev. C* **83**, 034907 (2011) [arXiv:1007.0130 [nucl-th]].
- [19] M. Martinez and M. Strickland, “Dissipative Dynamics of Highly Anisotropic Systems,” *Nucl. Phys. A* **848**, 183 (2010) [arXiv:1007.0889 [nucl-th]].
- [20] T. Schäfer, “Dissipative fluid dynamics for the dilute Fermi gas at unitarity: Free expansion and rotation,” *Phys. Rev. A* **82**, 063629 (2010) [arXiv:1008.3876 [cond-mat.quant-gas]].

- [21] K. Dusling and T. Schäfer, “Elliptic flow of the dilute Fermi gas: From kinetics to hydrodynamics,” *Phys. Rev. A* **84**, 013622 (2011) [arXiv:1103.4869 [cond-mat.stat-mech]].
- [22] C. Menotti, P. Pedri, S. Stringari, “Expansion of an interacting Fermi gas,” *Phys. Rev. Lett.* **89**, 250402 (2002) [cond-mat/0208150].
- [23] P. Pedri, D. Guéry-Odelin and S. Stringari, “Dynamics of a classical gas including dissipative and mean-field effects,” *Phys. Rev. A* **68**, 043608 (2003) [cond-mat/0305624].
- [24] S. Chiacchiera, D. Davesne, T. Enss, and M. Urban, “Damping of the quadrupole mode in a two-dimensional Fermi gas,” *Phys. Rev. A* **88**, 053616 (2013) [arXiv:1309.3651 [cond-mat.quant-gas]].
- [25] P. A. Pantel, D. Davesne and M. Urban, “Numerical solution of the Boltzmann equation for trapped Fermi gases with in-medium effects,” *Phys. Rev. A* **91**, 013627 (2015) [arXiv:1412.3641 [cond-mat.quant-gas]].
- [26] P. Colella, P. R. Woodward, “The Piecewise Parabolic Method (PPM) for Gas-Dynamical Simulations,” *J. Comp. Phys.* **54**, 174 (1984).
- [27] J. M. Blondin, E. A. Lufkin, “The piecewise-parabolic method in curvilinear coordinates,” *Astrophys. J. Supp. Ser.* **88**, 589 (1993).
- [28] J. Chao and T. Schäfer, “Conformal symmetry and non-relativistic second order fluid dynamics,” *Annals Phys.* **327**, 1852 (2012) [arXiv:1108.4979 [hep-th]].
- [29] T. Schäfer, “Second order fluid dynamics for the unitary Fermi gas from kinetic theory,” *Phys. Rev. A* **90**, 043633 (2014) [arXiv:1404.6843 [cond-mat.quant-gas]].